



Study Of The Effect Of Annealing Time On CuO/NiO P-Type MSM Photodetector Prepared By A Thermal Vacuum Evaporation Method.

Abdulrahman Rashid Hammood ^{1*}, N.K. Hassan ², Abdul Kareem Dahash Ali ³

¹*university of Tikrit, Iraq, Email: abdulrahmman002@gmail.com

²university of Tikrit, Iraq, Email: nadimkh4@tu.edu.iq

***Corresponding Author:** - Abdulrahman Rashid Hammood

*University of Tikrit, Iraq, Email: abdulrahmman002@gmail.com

Abstract

Copper oxide/nickel oxide (CuO/NiO) thin films deposited on glass substrates by Physical vapor deposition (PVD) Technique and then annealed at 360°C for different annealing times (one hour, one and half hours, and two hours). The effects of the annealing time on the structural, optical, and electrical properties of the CuO/NiO thin films were studied. X-ray diffraction suggests that a Monoclinic and cubic structure with a strong (1 1 1) and (2 2 0) for each of CuO and NiO respectively preferred orientation which remained the same with different heat treatments. and the crystallite size increases with increasing annealing times, it is found that with the increase of different time treatments, The optical absorption spectra showed that increasing annealing time, The absorption peak continues to decrease with increasing annealing time to become 0.74 with a slight shift towards the shorter wavelength Absorbance. the band gap of about 2.90 eV at 1 h and 1.5 h has 2.86 eV. For 2 h annealed films, the optical band gap continues to decrease close to 2.74 eV. Our results showed that the photo response properties of the photodetectors are strongly dependent on the surface-to-volume ratio. The annealing time enhanced photodetection performance, high sensitivity, and shortened rise times We showed that photodetectors annealed for two hours have a faster response than the other.

Keywords: nickel oxide, annealing times, physical vapor deposition, thin film, copper oxide, thermal vacuum evaporation.

Introduction

Due to their structural, optical, and electrical properties, copper oxide (CuO) and nickel oxide (NiO) are both significant p-type semiconductors that have recently gained significant attention from researchers. [1, 2] It has a cubic rock salt-like structure with octahedral Ni²⁺ and O²⁻ sites, making nickel oxide (NiO) a unique semitransparent semiconducting material.[3] Wide band gap semiconductors made of nickel oxide have exceptional features, including great chemical and mechanical stability, extreme stability across a wide temperature range, and a direct band gap. [4]. Due to the multivalent nature of copper, copper oxide exists in two common crystalline forms: cupric oxide (tenorite monoclinic CuO) and cuprous oxide (cuprite cubic Cu₂O), both of which are semiconductors with bandgap energies ranging from (1.3 to 2.1 and 2.1 to 2.6 eV), respectively. [5 6]. Furthermore, various studies into similar applications have been done on NiO, CuO, and Cu₂O. such as photocatalysts[7] [8], [9], gas sensors[10,11, 12], photodetectors[13] [14, 15], and solar cells[16 ,17, 18],. several methods, including evaporation [19, 20], sol-gel [21 22] spray pyrolysis [23,24], and physical vapor deposition methods had been employed to synthesize CuO / NiO films.

Materials and Methods

After cleaning the glass slides that measured (76x21x1) millimeters, with distilled water and ethanol, followed by drying and wiping with optical cleaning paper nickel (Ni) metal are used in the form of a powder with a purity of 99%, and copper (Cu) metal in the form of a powder with a purity of 99%, we use a physical vapor deposition device as shown in (Fig.1). To precipitate a thin film of nickel (Ni), The process takes place under reduced pressure about(2x10⁻⁵ m bar)the precipitated films are then annealed at 360 C at different times (1hou, 1.5 hours, and 2hours) to convert them to nickel oxide (NiO) Then we return the better nickel oxide (NiO) thin film to the physical vapor deposition device and we put copper (Cu) metal in the crucible and evaporate the copper and annealing it to obtain a thin film of copper oxide/nickel oxide (CuO/NiO).

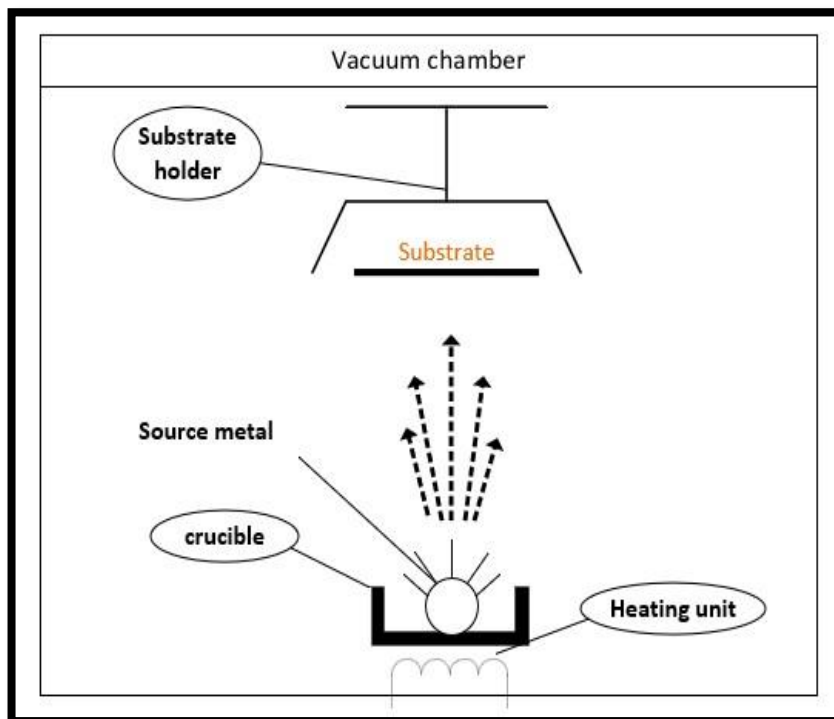


Figure 1: Schematic illustration of physical vapor deposition-PVD-process

Results and Discussions

Structure and morphology of the CuO/NiO films. The structure of the CuO/NiO films and the growth films can be identified by comparing the X-ray diffraction measurement data to the ASTM (American Society of Testing Materials) cards.). (Fig.2) illustrates the x-ray diffraction patterns of CuO/NiO thin films that were annealed at 360 °C temperatures for different periods of time (1 hour, 1.5 hours, and 2 hours). at an annealing time of 1 h we obtained on ten peaks of Tenorite

CuO at diffraction angles of {32.27, 35.25, 38.51, 46.17, 48.51, 51.238, 53.32, 58.29, 61.50, 72.288, and 79.82,} corresponding to {(1 1 0), (0 0 2), (1 1 1), (-1 1 2), (-2 0 2), (1 1 2), (0 2 0), (2 0 2), (-1 1 3), (3 1 1) and (0 2 3)} with Monoclinic structure and pattern of Bunsénite NiO at diffraction angles {37.46, 43.44, 63.19, 75.40 and 79.82} corresponding to {(1 1 1), (2 0 0), (2 2 0), (3 1 1) and (2 2 2)} with cubic structure at an annealing time of 1.5 h, XRD peaks obtained show that films have a polycrystalline structure with single-phase Tenorite CuO with Monoclinic structure at diffraction angles of {32.27, 35.25, 38.51, 46.81, 48.63, 51.23, 53.32, 58.26, and 61.23}, corresponding to the crystal planes {(1 1 0), (0 0 2), (1 1 1), (-1 1 2), (-2 0 2), (1 1 2), (0 2 0), (2 0 2) and (-1 1 3)} and NiO with cubic structure at diffraction angles of {37.46, 43.44, 63.32, 75.40, and 79.16,} corresponding to the planes{(1 1 1), (2 0 0), (2 2 0), (3 1 1) and (2 2 2)} and the films annealed at 2 h we obtained on ten peaks of Tenorite CuO at diffraction angles of {32.13, 35.25, 38.51, 46.17, 48.63, 51.23, 53.32, 58.26, 61.23, 72.16, and 73.07} corresponding to {(1 1 0), (-1 1 1), (1 1 1), (-1 1 2), (-2 0 2), (1 1 2), (0 2 0), (2 0 2), (-1 1 3), (3 1 1) and (2 2 1)} with Monoclinic structure and pattern of Bunsénite NiO at diffraction angles {37.46, 43.44, 63.19, 75.40 and 79.31} corresponding to {(1 1 1), (2 0 0), (2 2 0), (3 1 1) and (2 2 2)} with cubic structure When increasing the annealing time, we find that the intensity of the peaks increases with the dominant crystal orientation of the copper oxide (1 1 1) corresponding to the diffraction angle (38.6363) with COD File (No. 01-078-0428) and intensity of the nickel oxide peaks in a preferred direction (2 2 0) corresponding to the diffraction angle (63.1976) with COD File (No. 00-001-1239). indicates an increase in the crystallinity of the material and the regularity of its crystalline structure, which gives a greater opportunity for constructive interference to occur as a result of achieving the Bragg's condition for diffraction.

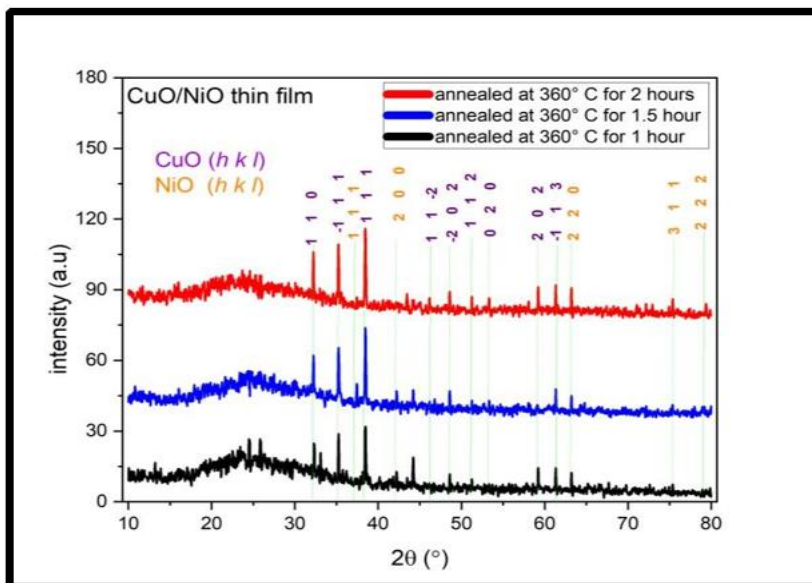
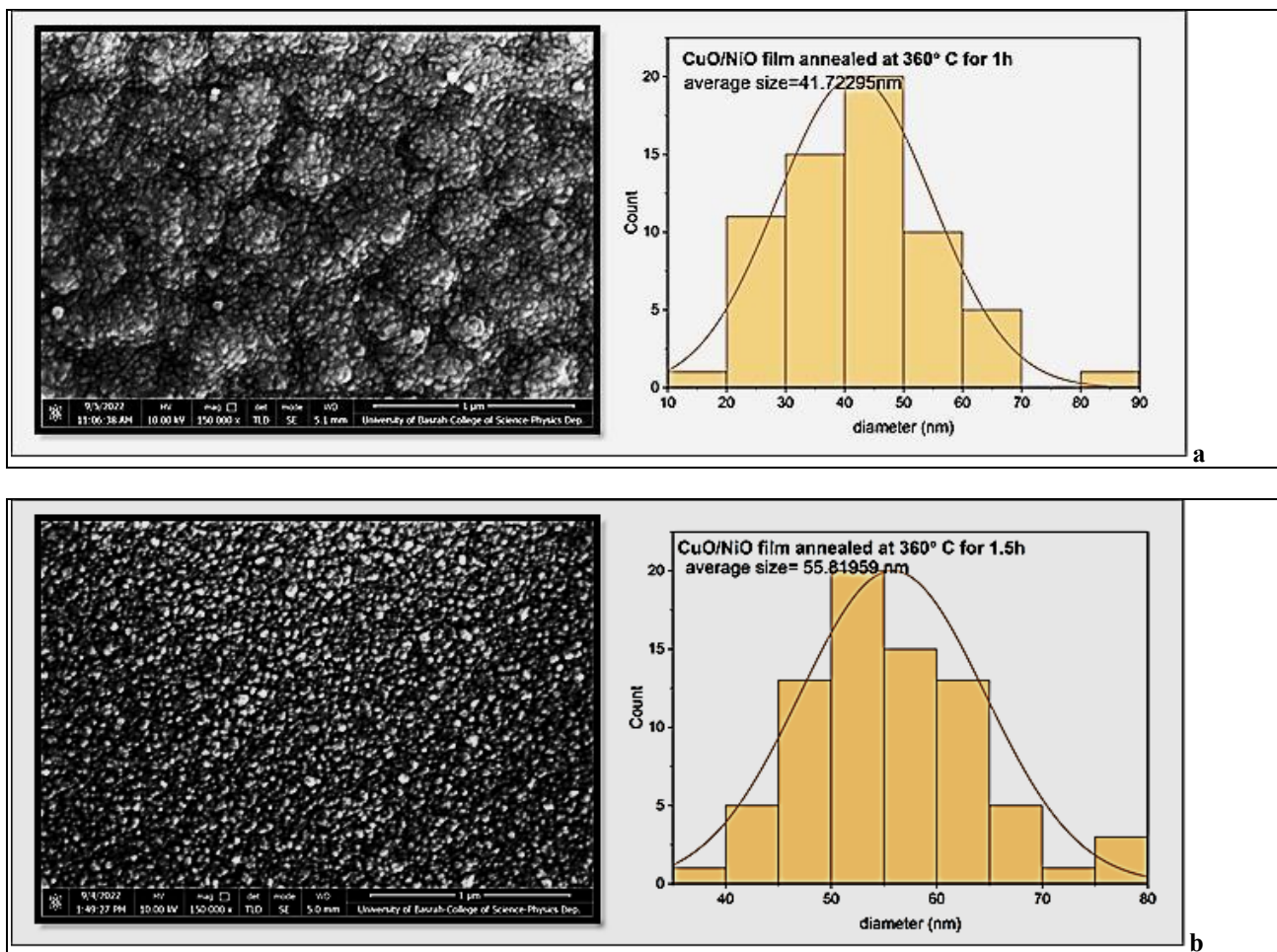


Figure 2: XRD spectra of CuO/NiO annealed at 360 °C with a different time of annealing

The morphology of the films was characterized using SEM at a 10 keV operating voltage (Fig.3) shows typical SEM images of CuO/NiO nanocomposite thin films grown on glass substrates with varying annealing periods. The findings demonstrated that the CuO/NiO thin layer has a fine nanoparticle structure and is prone to aggregate because of the homogeneity of the nanoparticles' surfaces and their high surface energy and surface tension. and is evenly diffused across all substrates. With The CuO/NiO films' grain size increases with longer annealing durations, as seen in (Fig.3 a, b, and c) , Continuous grain distribution shows that the grains cling properly to the prepared films' surface.



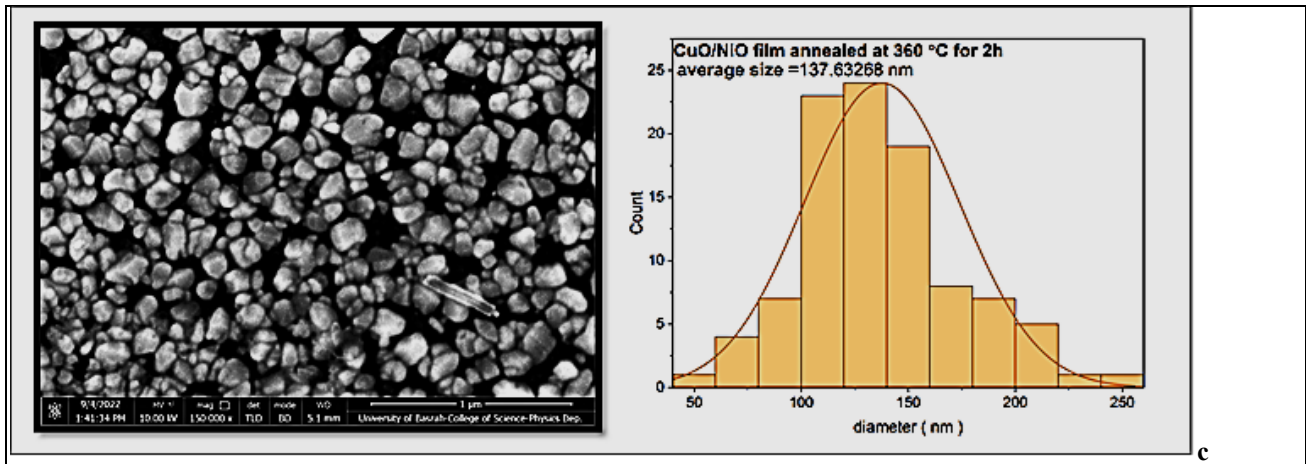


Figure 3: illustrates the surface morphology of CuO/ NiO thin film annealed at 360 °C a- annealed for one-hour b- annealed for one and half hours c- annealed for two hours **Optical properties.** optical transmission of annealed thin films was measured using a shimadzu

UV-1800 device in the UV-VIS region (300 - 1100 nm). For CuO/NiO films the optical band gap (E_g) is related by the direct band gap structure or direct transition semiconductors.[25]

$$\alpha = (h\nu - E_g)^{1/2} \quad (1)$$

h is Plank’s constant and ν is the frequency of the incident photon.

The absorbance spectra for CuO/NiO thin films with different annealing times at temperatures of 360C (300nm and 1100nm) were recorded and compared as demonstrated in (Fig.4). It is observed from the figure that the peak of absorption is about 1.67 at 340 nm wavelength at an annealing time of 1 h With an increase in the annealing time to an hour and a half, the absorption peak becomes approximately 0.85 at the same wavelength The absorption peak continues to decrease with increasing annealing time to become 0.74 with a slight shift towards the shorter wavelength Absorbance also decreases with increasing wavelength, and the decrease is observed between (340 and 530)nm approximately Which means that increasing the annealing time leads to a decrease in surface roughness, giving sufficient time for crystal growth, and increasing the size of the grains, which causes an increase in the membrane permeability and a decrease in the absorbance

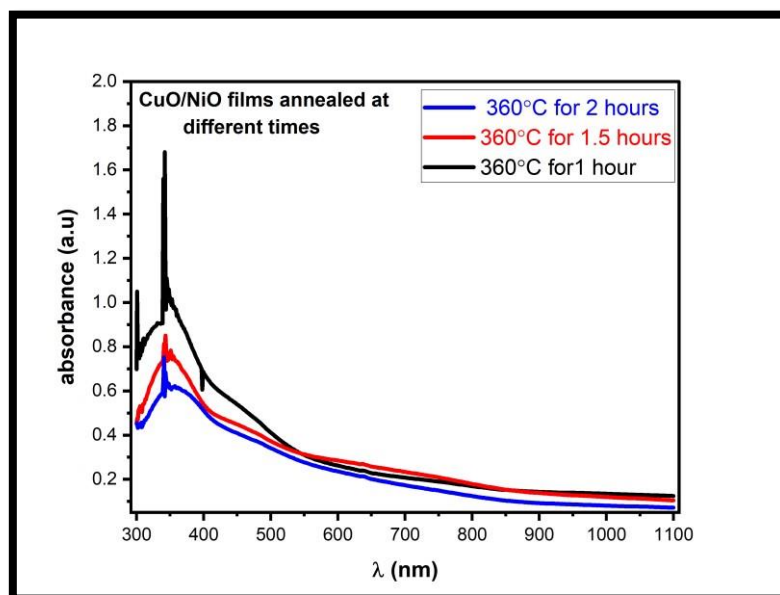


Figure 4: shows the relationship between absorbance as a function of wavelength of CuO/NiO films annealed at 360°C/1h ,360°C/1.5h and 360°C/2h

Equation (1) can be used to calculate optical energy gab For CuO/NiO thin films annealed at different times for the same temperatures, the value of the optical band gap has been determined from the value of the intercept of the straight line at

$\alpha = 0$. The films as deposited and annealed at 1 h have a band gap of about 2.90 eV and 1.5 h has 2.86 eV. For 2 h annealed films, the optical band gap continues to decrease close to 2.74 eV. The result is given in (Fig.5).

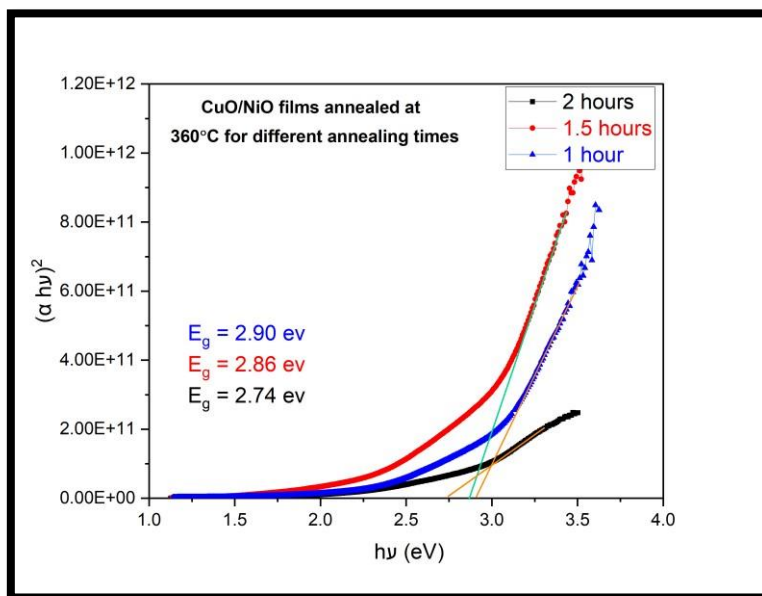


Figure 5: Tauc plots of the CuO/NiO thin film annealing at different times

Electrical properties. The following thermionic emission theory equations provide a good fit for the I-V curves and may be used to calculate the ideality factor and Schottky barrier height of manufacturing MSM[26,27]

$$I = I_{s0} \left(e^{\frac{-qV}{\beta k_B T}} - 1 \right) \tag{2}$$

where I_{s0} is the saturation current given by:

$$I_{s0} = AA^*T^2 e^{\frac{-q\phi_B}{k_B T}} \tag{3}$$

where A^* is the effective Richardson constant, A is the Schottky contact area, q is the charge of an electron, T is the absolute temperature, k_B is the Boltzmann constant, ϕ_B is the barrier height and β is the ideality factor. which is obtained by rearranging (Equation 6)

$$\beta = \frac{q}{k_B T} \left[\frac{V_F}{\ln \frac{I_F}{I_{s0}}} \right] \tag{4}$$

where V_F is the forward bias voltage, I_F and I_{s0} are the forward bias current.

The relationship between the voltage applied and the current passing through the CuO/NiO MSM detector after it has been annealed at 360°C for various lengths of time with Al electrodes is shown in (Fig. 6). The voltage measurements were carried out with a bias voltage of (5 Volt) supplied. The current of CuO/NiO MSM detectors at the various annealing times in the forward bias is found to be (2.52, 2.7, and 5.15 nA., respectively) based on the relationship between current and voltages. In the CuO/NiO thin films, the current is higher than after increasing the annealing time because the structural properties of the thin film have been improved, resulting in a tiny energy gap. Since electrons require less energy to bridge the energy gap, this is why the current is higher. Make the inference from the findings that the diode material exhibits the relationship between current and voltages for prepared samples.

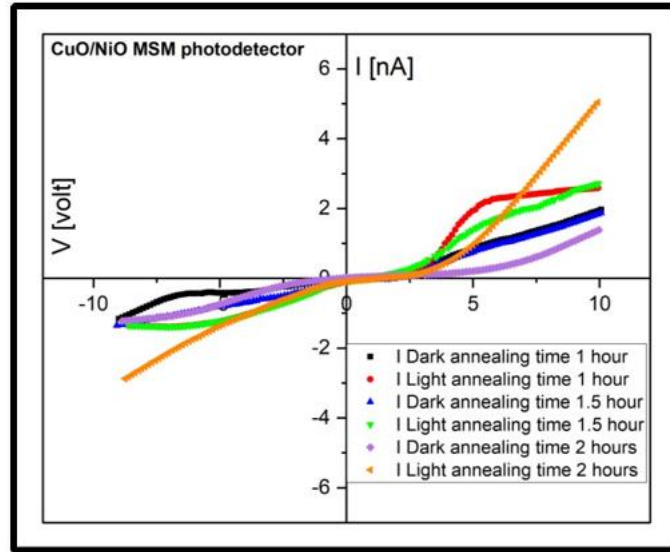


Figure 6: The Current – Voltage comparison between Dark and Light of CuO/NiO thin film deposited glass substrate annealed at 360°C for different annealing time

By evaluating the photo response using dynamic responsivity time measurement through illuminating sensors to chop light at 5 V, the repeatability of the CuO/NiO MSM device was explored in (Fig. 3). Large photoactive surface areas, great quality, and a lack of defects were all factors that contributed to MSM's positive response. [28, 29]. Due to the growing photocurrent, the voltage increased while the saturation current increased. For the thin film that was annealed at 360°C for 2 hours, the MSM device was more sensitive at 5 V. The applied electric field created photo-generated charges while the PD was illuminated. The device's conductivity was then effectively increased by the photocurrent in conjunction with the bias current.[29]. As responsivity ($R\lambda$), quantum efficiency ($\eta(\lambda)$), noise equivalent power (NEP), and specific detectivity (D^*) are measured at various temperatures, other electrical parameters of the photodetector made from annealed CuO/NiO are investigated. as demonstrated in (table .1)

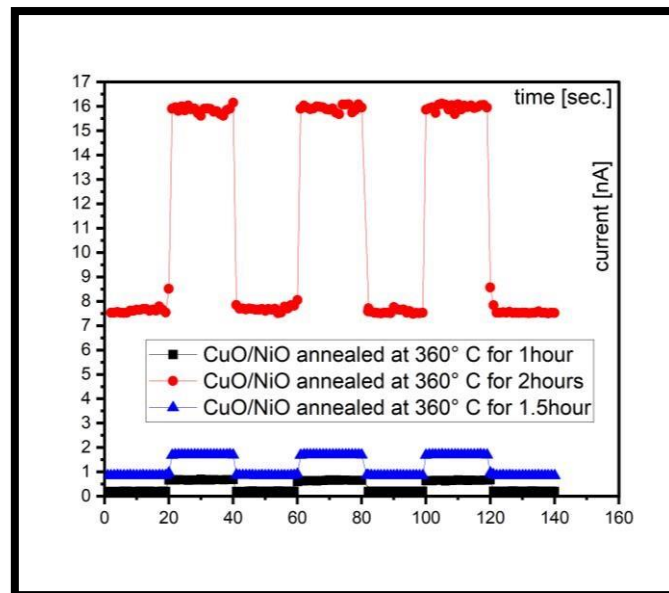


Figure 7: The repetitive switching of the light for the CuO/NiO photodiode devices at $V = 5$ V

Table 1: Results of photodetectors for CuO/NiO thin films illumination at 450 nm.

Sample Thin film	annealing conditions		$R\lambda$ [$10^{-6}A/W$]	$\eta(\lambda)\%$	NEPx10-10 [W]	$D^* \times 10^8$ [$Hz^{1/2}. W^{-1}$]	[cm.]
	annealing time [hour]	Annealing temperatures[°C]					
CuO/NiO	1	360	2.53	0.00071	4.34	5.66	
	1.5	360	2.6	0.00073	4.04	6.19	
	2	360	1.48	0.00041	3.87	6.49	

Conclusions.

Nanocrystalline CuO/NiO thin films were successfully deposited on a glass substrate using an effective, less complicated, and more economical PVD process. The produced films are uniformly structured and adhered to the substrate. According to the XRD results, the intensity and crystallite size increase as the annealing period increases. The morphological results showed that the grains are well distributed over the substrate and the films have a high homogeneity layer with the sizes of (41.72, 55.81 and 137.63) nm. Also, with more annealing time, the optical energy gap was found to be less ($E_g = 2.90, 2.86, \text{ and } 2.74$) eV for annealing times of (1 hour, 1.5 hours, and 2 hours), respectively. These films are useful for nano-optoelectronic applications, particularly in the solar cell as a window or antireflection due to their high transparency and wide band gap properties. High photodetection performance was achieved by increasing annealing time which led to enhanced sensitivity and faster response to illumination. The origin of these behaviors is related to the enhancement of the surface-to-volume ratio.

References

- [1] W. J. Lee and X. J. Wang, "Structural, optical, and electrical properties of copper oxide films grown by the silar method with post-annealing," *Coatings*, vol. 11, no. 7, Jul. 2021, doi: 10.3390/coatings11070864.
- [2] V. P. Patil *et al.*, "Effect of Annealing on Structural, Morphological, Electrical and Optical Studies of Nickel Oxide Thin Films," *J Surf Eng Mater Adv Technol*, vol. 01, no. 02, pp. 35–41, 2011, doi: 10.4236/jsemat.2011.12006.
- [3] M. Aftab, M. Z. Butt, D. Ali, F. Bashir, and T. M. Khan, "Optical and electrical properties of NiO and Cu-doped NiO thin films synthesized by spray pyrolysis," *Opt Mater (Amst)*, vol. 119, Sep. 2021, doi: 10.1016/j.optmat.2021.111369.
- [4] M. M. Gomaa, M. H. Sayed, V. L. Patil, M. Boshta, and P. S. Patil, "Gas sensing performance of sprayed NiO thin films toward NO₂ gas," *J Alloys Compd*, vol. 885, Dec. 2021, doi: 10.1016/j.jallcom.2021.160908.
- [5] D. S. Murali, S. Kumar, R. J. Choudhary, A. D. Wadikar, M. K. Jain, and A. Subrahmanyam, "Synthesis of Cu₂O from CuO thin films: Optical and electrical properties," *AIP Adv*, vol. 5, no. 4, Apr. 2015, doi: 10.1063/1.4919323.
- [6] A. A. Ogwu, T. H. Darma, and E. Bouquerel, "Electrical resistivity of copper oxide thin films prepared by reactive magnetron sputtering," 2007. [Online]. Available: www.journalamme.org
- [7] B. Mustafa Naeem Husain Waked Supervisor Iyad Saadeddin Co-Supervisor Mohammed Suleiman Shtaya, "Faculty of Graduate Studies," 2017.
- [8] J. Yu, Y. Hai, and M. Jaroniec, "Photocatalytic hydrogen production over CuO-modified titania," *J Colloid Interface Sci*, vol. 357, no. 1, pp. 223–228, May 2011, doi: 10.1016/j.jcis.2011.01.101.
- [9] N. D. Khiavi, R. Katal, S. K. Eshkalak, S. Masudy-Panah, S. Ramakrishna, and H. Jiangyong, "Visible light driven heterojunction photocatalyst of cuo-cu₂o thin films for photocatalytic degradation of organic pollutants," *Nanomaterials*, vol. 9, no. 7, Jul. 2019, doi: 10.3390/nano9071011.
- [10] G. Tan, D. Tang, X. Wang, L. He, T. Mu, and G. Li, "Preparation of NiO Thin Films and Their Application for NO₂ Gas Detection," *Int J Electrochem Sci*, vol. 17, 2022, doi: 10.20964/2022.05.45.
- [11] A. Rydosz, "The use of copper oxide thin films in gas-sensing applications," *Coatings*, vol. 8, no. 12. MDPI AG, Dec. 01, 2018. doi: 10.3390/coatings8120425.
- [12] S. Steinhauer, "Gas sensors based on copper oxide nanomaterials: A review," *Chemosensors*, vol. 9, no. 3. MDPI AG, pp. 1–20, Mar. 01, 2021. doi: 10.3390/chemosensors9030051.
- [13] M. El-Kemary, N. Nagy, and I. El-Mehasseb, "Nickel oxide nanoparticles: Synthesis and spectral studies of interactions with glucose," *Mater Sci Semicond Process*, vol. 16, no. 6, pp. 1747–1752, 2013, doi: 10.1016/j.mssp.2013.05.018.
- [14] S. B. Wang *et al.*, "A CuO nanowire infrared photodetector," *Sens Actuators A Phys*, vol. 171, no. 2, pp. 207–211, Nov. 2011, doi: 10.1016/j.sna.2011.09.011.
- [15] A. M. Selman, M. A. Mahdi, and Z. Hassan, "Fabrication of Cu₂O nanocrystalline thin films photosensor prepared by RF sputtering technique," *Physica E Low Dimens Syst Nanostruct*, vol. 94, pp. 132–138, Oct. 2017, doi: 10.1016/j.physe.2017.08.007.
- [16] S. K. Kim *et al.*, "Comparison of NiO: Xthin film deposited by spin-coating or thermal evaporation for application as a hole transport layer of perovskite solar cells," *RSC Adv*, vol. 10, no. 71, pp. 43847–43852, Nov. 2020, doi: 10.1039/d0ra08776a.
- [17] T. Oku, T. Yamada, K. Fujimoto, and T. Akiyama, "Microstructures and photovoltaic properties of Zn(Al)O/Cu₂O-based solar cells prepared by spin-coating and electrodeposition," *Coatings*, vol. 4, no. 2, pp. 203–213, Jun. 2014, doi: 10.3390/coatings4020203.
- [18] Y. Alajlani, F. Placido, H. O. Chu, R. de Bold, L. Fleming, and D. Gibson, "Characterisation of Cu₂O/CuO thin films produced by plasma-assisted DC sputtering for solar cell application," *Thin Solid Films*, vol. 642, pp. 45–50, Nov. 2017, doi: 10.1016/j.tsf.2017.09.023.
- [19] B. Sasi, K. G. Gopchandran, P. K. Manoj, P. Koshy, P. Prabhakara Rao, and V. K. Vaidyan, "Preparation of transparent and semiconducting NiO films," 2003.
- [20] B. Balamurugan and B. R. Mehta, "Optical and structural properties of nanocrystalline copper oxide thin films prepared by activated reactive evaporation," 2001.
- [21] "Nickel oxide sol-gel films from nickel diacetate for electrochromic".

- [22] Z. N. Kayani, M. Umer, S. Riaz, and S. Naseem, "Characterization of Copper Oxide Nanoparticles Fabricated by the Sol–Gel Method," *J Electron Mater*, vol. 44, no. 10, pp. 3704– 3709, Oct. 2015, doi: 10.1007/s11664-015-3867-5.
- [23] J. D. Desai, S. K. Min, K. D. Jung, and O. S. Joo, "Spray pyrolytic synthesis of large area NiO x thin films from aqueous nickel acetate solutions," *Appl Surf Sci*, vol. 253, no. 4, pp. 1781–1786, Dec. 2006, doi: 10.1016/j.apsusc.2006.03.009.
- [24] Y. Zhu, Z. Xu, K. Yan, H. Zhao, and J. Zhang, "One-Step Synthesis of CuO-Cu₂O Heterojunction by Flame Spray Pyrolysis for Cathodic Photoelectrochemical Sensing of l Cysteine," *ACS Appl Mater Interfaces*, vol. 9, no. 46, pp. 40452–40460, Nov. 2017, doi: 10.1021/acsami.7b13020.
- [25] J. F. Mohammad, M. A. A. Sooud, and S. M. Abed, "CHARACTERISTICS OF pH VARIATION ON STRUCTURAL AND OPTICAL PROPERTIES OF NANOCRYSTALLINE SnO₂ THIN FILMS BY CBD TECHNIQUE."
- [26] B. B. Eneaze Al-Jumaili, Z. A. Talib, J. L. Y, S. B. Paiman, and N. M. Ahmed, "Photoelectric properties of Metal-Semiconductor-Metal Photodetector based on Porous Silicon," 2016. [Online]. Available: <http://letters.masshp.net/ISSN0128-8393>
- [27] N. K. Hassan, M. R. Hashim, K. Al-Heuseen, and N. K. Allam, "Interface architecture determined the performance of ZnO nanorods-based photodetectors," *Chem Phys Lett*, vol. 604, pp. 22–26, Jun. 2014, doi: 10.1016/j.cplett.2014.05.001.
- [28] H. R. Abd, Y. Al-Douri, N. M. Ahmed, and U. Hashim, "Alternative-current electrochemical etching of uniform porous silicon for photodetector applications," *Int. J. Electrochem. Sci*, vol. 8, pp. 11461–11473, 2013.
- [29] A. M. Selman and Z. Hassan, "Highly sensitive fast-response UV photodiode fabricated from rutile TiO₂ nanorod array on silicon substrate," *Sens Actuators A Phys*, vol. 221, pp. 15–21, 2015.